

TopoReformer: Mitigating Adversarial Attacks Using Topological Purification in OCR Models

Bhagyesh Kumar*, A S Aravinthakashan*, Akshat Satyanarayan*, Ishaan Gakhar, Ujjwal Verma

Manipal Institute of Technology, Manipal Academy of Higher Education Manipal - 576104, India
invi.bhagyesh@gmail.com, aravinthakshanmain@gmail.com, pkmnakshat@gmail.com, ishaangakhar04@gmail.com,
ujjwal.verma@manipal.edu

Abstract

Adversarially perturbed images of text can cause sophisticated OCR systems to produce misleading or incorrect transcriptions from seemingly invisible changes to humans. Some of these perturbations even survive physical capture, posing security risks to high-stakes applications such as document processing, license plate recognition, and automated compliance systems. Existing defenses, such as adversarial training, input preprocessing, or post-recognition correction, are often model-specific, computationally expensive, and affect performance on unperturbed inputs while remaining vulnerable to unseen or adaptive attacks. To address these challenges, *TopoReformer* is introduced, a model-agnostic reformation pipeline that mitigates adversarial perturbations while preserving the structural integrity of text images. Topology studies properties of shapes and spaces that remain unchanged under continuous deformations, focusing on global structures such as connectivity, holes, and loops rather than exact distance. Leveraging these topological features, *TopoReformer* employs a topological autoencoder to enforce manifold-level consistency in latent space and improve robustness without explicit gradient regularization. The proposed method is benchmarked on EMNIST, MNIST, against standard adversarial attacks (FGSM, PGD, Carlini-Wagner), adaptive attacks (EOT, BDPA), and an OCR-specific watermark attack (FAWA).

Code — <https://github.com/invi-bhagyesh/TopoReformer>

Introduction

The widespread adoption of OCR in critical safety and compliance workflows, such as document automation (Karthikeyan et al. 2021), traffic enforcement (Kakani, Gandhi, and Jani 2017), and enterprise data extraction (Bazzo et al. 2020), means that even minor transcription errors can propagate to financial loss (Pingili 2025), policy breaches, or wrongful enforcement actions at scale. This dependence on OCR has grown with the broad adoption of deep neural networks (DNNs) (Akhtar and Mian 2018), which have significantly advanced recognition accuracy and enabled deployment in many high-stakes applications. However, OCR also inherits the security vulnerabilities of DNNs

(Li et al. 2022). It is highly susceptible to adversarial examples, where human imperceptible perturbations to text images can cause targeted or severe transcription errors, even surviving real-world channels such as print and scan or display and camera capture.

These developments underscore a fundamental challenge for which various defense strategies have been explored to counter this threat. In general, the domain of adversarial defense has followed four directions: preprocessing through purification or denoising modules that project inputs back into a learned data manifold (Meng and Chen 2017) (Hwang et al. 2019); detection of anomalous inputs (He et al. 2022), often via autoencoder-based reconstruction errors (Cintas et al. 2021) or distributional tests (Folz et al. 2020); adversarially robust training of recognition models (Zhao, Alwidian, and Mahmoud 2022), (Qian et al. 2022); and post-processing corrections applied to suspicious text (Xie et al. 2017), (Imam, Vassilakis, and Kolovos 2022). However, these approaches remain costly, model-specific, or prone to failure on unseen attacks, motivating the need for more generalizable defenses. To address these limitations, *TopoReformer* is proposed, which is designed as a cost-alleviating, model-agnostic framework that maintains robustness even against adaptive attacks. The proposed approach operates independently of specific OCR architectures and avoids adversarial retraining, thus ensuring scalability and ease of deployment while providing stable defense across a wide range of perturbation types.

Topology (Edelsbrunner, Harer et al. 2008) studies the properties of shapes and spaces that remain unchanged under continuous deformations, focusing on global structures such as connectivity, holes, and loops rather than exact distances. This invariance forms the core intuition behind the proposed approach: adversarial perturbations often distort only local pixel relationships, whereas the overall topological structure of the data remains intact. By embedding this structural prior into the learning process through their loss function, topological autoencoders naturally filter out such perturbations and recover the underlying manifold of clean samples. *TopoReformer*, unlike denoising-based defenses that rely solely on pixel-level reconstruction (Meng and Chen 2017), uses an additional topological loss that enforces consistency between the persistent homology of the

*These authors contributed equally.

input and its latent representation.

TopoReformer distinguishes itself from denoising models or obfuscated gradients, which were used repeatedly in many adversarial robustness papers and shown to provide a false sense of "robustness" (Athalye, Carlini, and Wagner 2018). The reshaped manifold thus performs purification, not denoising, discarding perturbations that do not correspond to meaningful topological variations—a distinction validated experimentally under adaptive attacks. The novelty of this work lies in a topology-based purification method that addresses watermark-based OCR attacks, adaptive and classical adversarial attacks such as EOT (Athalye et al. 2018), BPDA (Athalye, Carlini, and Wagner 2018), Carlini (Carlini and Wagner 2017), PGD (Madry et al. 2017), and FGSM (Goodfellow, Shlens, and Szegedy 2014), trained solely on unperturbed data without adversarial examples. Experimental results demonstrate that the approach effectively removes adversarial artifacts, underscoring the distinctive inductive bias underlying the method.

Although some work has explored the use of topological features in related contexts (Goibert, Ricatte, and Dohmatob 2022; Gebhart and Schrater 2017), the literature on topological autoencoders to mitigate adversarial attacks remains very limited. For example, (Vu et al. 2025) leverages topological features for logit alignment, and (Kuang et al. 2024) applies topological methods for adversarial defense. However, there appears to be little to no prior work employing topological autoencoders for end-to-end purification or defense. To the best of the authors' knowledge, this work is the first to employ Topological Autoencoders in this setting. The main contributions of the paper are summarized as follows:

- **Topological purification:** A Topological Autoencoder is employed for the purification of adversarial images, followed by a lightweight reformer trained on unperturbed data. This setup suppresses adversarial artifacts while preserving the overall structure of the inputs toward a cleaner manifold.
- **Freeze-Flow training paradigm:** A novel training scheme that blocks direct gradients to the primary encoder and routes them through an auxiliary module, encouraging reliance on topology-consistent latents to complement the purification, yielding up to 5% improvement in classification performance under Carlini-Wagner attacks.
- **Model Agnostic OCR defense :** A drop-in, model-agnostic pipeline for any OCR model that integrates the topology-guided purifier and Reformer, providing robustness against white-box, black-box, and adaptive attacks without requiring adversarial training.

Related Works

The following subsections frame the problem space by first motivating the choice of adversarial attacks as representative benchmarks. Next, reconstruction-based reformers (purifiers), such as denoising and masked autoencoders, are reviewed with an emphasis on their limitations. Finally, topology-preserving autoencoders are introduced, highlighting their motivation in guiding the proposed pipeline.

Adversarial Attacks

Adversarial attacks (Chakraborty et al. 2021) are deliberate, minimal perturbations to inputs or training data crafted to induce a model to produce incorrect, unintended, or targeted outputs while remaining imperceptible to humans. In evaluation, they are typically framed as worst-case, bounded perturbations that maximize a loss (untargeted) or enforce a specific prediction (targeted) under white, gray, or black-box conditions. FGSM (Goodfellow, Shlens, and Szegedy 2014) applies a single-step gradient-sign update to reveal linearity-driven vulnerabilities, while PGD (Madry et al. 2017) extends this into iterative projected updates within a bounded norm, becoming the de facto standard for robustness evaluation and adversarial training. C&W (Carlini and Wagner 2017) formulates adversarial generation as an optimization problem minimizing perturbation magnitude subject to a confidence-based misclassification constraint, producing high-confidence, low-distortion examples that have historically bypassed many defenses.

Later, it was highlighted that several defenses evaluated only against such static attacks (Athalye, Carlini, and Wagner 2018) achieved a false sense of security due to gradient obfuscation, non-differentiable, randomized, or poorly conditioned transformations that blocked adequate gradient flow. Adaptive attacks were proposed to address this, where the adversary explicitly models or approximates the defense during optimization. Two major frameworks, Backward Pass Differentiable Approximation (BPDA) (Athalye, Carlini, and Wagner 2018) and Expectation over Transformation (EOT) (Athalye et al. 2018), emerged as standard. BPDA substitutes non-differentiable components with differentiable surrogates during backpropagation, while EOT estimates expected gradients over stochastic transformations. This ensures that evaluations assess actual robustness rather than artifacts of gradient masking.

Autoencoder-based Reformers and Defenses

Denoising autoencoder-based purifiers aim to reconstruct inputs to remove perturbations before classification. Methods such as PuVAE (Hwang et al. 2019), APuDAE (Kalaria, Hazra, and Chakrabarti 2022), and MAEP (Chen and Lu 2025) improve performance on MNIST, CIFAR-10, and ImageNet, but often degrade accuracy on unperturbed inputs (Yang et al. 2024). Earlier autoencoder-based defenses, such as (Meng and Chen 2017) and (Bakhti et al. 2019), also reform threshold input, but minor L1 perturbations can bypass them (Lu et al. 2018). Defenses that combine denoising with randomized transformations fail under adaptive attacks using Expectation Over Transformation (EOT), which averages over randomness to circumvent purifiers. Notable examples include (Dhillon et al. 2018; Xie et al. 2017; Guo et al. 2017), all of which saw their accuracy drop near 0% under EOT. In contrast, TopoReformer allows a classifier to make robust predictions even under adaptive attacks, with the help of global manifold preservation to maintain performance on both unperturbed and perturbed data, which is an issue with most adversarial-aware training paradigms that sacrifice performance on the unperturbed or clean samples in the attempt to perform well on adversarial inputs.

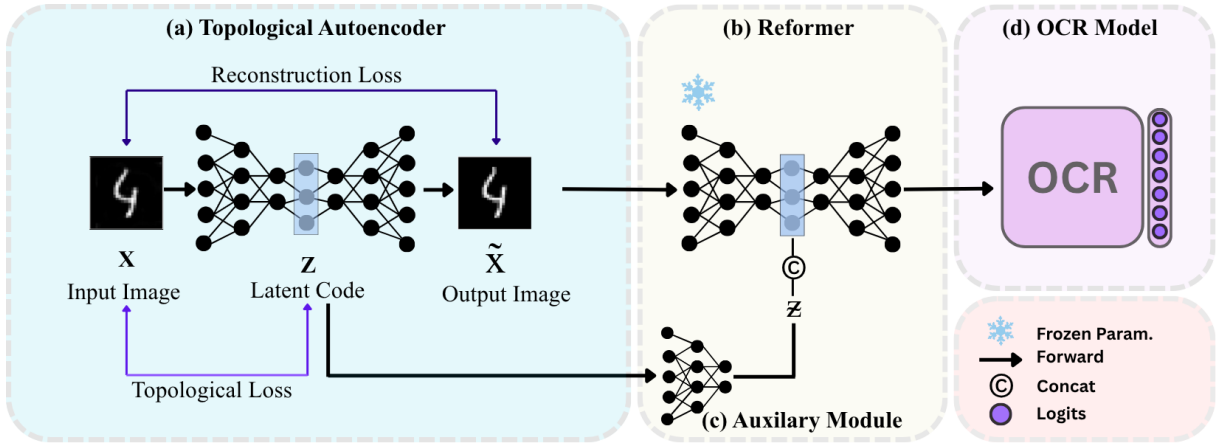


Figure 1: Schematic of the TopoReformer pipeline and the freeze-flow paradigm. The Topological Autoencoder (TopoAE), Auxiliary Module, and Reformer diagrams are illustrative and do not represent the actual neural network architectures.

Topological Autoencoders

Topology-preserving autoencoders (Moor et al. 2020) incorporate persistent-homology loss to retain the multiscale connectivity of inputs in latent or reconstructed spaces, preserving structural cues such as stroke and loop continuity, which are critical for optical character recognition. These autoencoders compute topological signatures for input and latent spaces, minimizing their discrepancy, producing representations that maintain global structure while achieving low reconstruction error on real image data. This provides a principled basis for structure-faithful purification without the need to retrain the classifier. Topological autoencoders have previously been applied for preserving structure representation learning (Sainburg, McInnes, and Gentner 2021), improving graph neural network embeddings (Horn et al. 2021), and detecting anomalies in physics (Ngairangbam et al. 2025) by capturing deviations from the learned topological manifold. No work has explored the use of topological autoencoders for adversarial defense or input purification.

Methodology

The methodology section is structured as follows: first, the Topological Autoencoder (TopoAE) is introduced along with a detailed discussion of persistent homology, persistence diagrams, and the associated topological loss. This is followed by a description of the Reformer module, the auxiliary model, the proposed training paradigm, and the visualization of the topological latent space.

A Topology-Preserving Autoencoder

The pipeline proposed, illustrated in Fig. 1, consists of three main components: the topological autoencoder (TopoAE), the Reformer (VAE), and the Auxiliary module. The input image is first processed by the TopoAE, which generates: a latent representation that encodes the topological structure of the input, and a reconstructed output (purified) that preserves the essential topological properties while filtering out topologically irrelevant variations. This purified image is

then passed through the Reformer, which adjusts the output of the TopoAE to better align with the expected manifold of the OCR model. Simultaneously, the latent vector is routed through the Auxiliary Module, which injects this topological information into the bottleneck of the Reformer. Finally, the decoder of the Reformer reconstructs the purified image, which is then passed to the downstream classifier for final transcription.

The central motivation behind this work lies in the working of the autoencoder based on *persistent homology* (Zomorodian and Carlsson 2004), a computational topology tool used to capture connectivity-based structures in data. Given a simplicial complex K , homology identifies d -dimensional features such as connected components ($d = 0$), loops ($d = 1$), and voids ($d = 2$). Instead of relying on a single complex, persistent homology tracks how these features appear and disappear across multiple scales using the Vietoris–Rips complex $R_\epsilon(X)$, built from pairwise distances within a point cloud X . As the scale (ϵ) increases, $R_\epsilon(X)$ expands and features merge or vanish, forming *persistence diagrams* D_d that record the birth and death of each topological feature. These diagrams are stable to small perturbations and can be compared via the bottleneck distance (Cohen-Steiner, Edelsbrunner, and Harer 2005). Persistent homology thus provides a multiscale, noise-robust summary of the data’s intrinsic topological structure, forming the basis for the topology-preserving autoencoder. The core idea is to compute persistence diagrams for both data and latent spaces and penalize their topological difference, encouraging multiscale connectivity patterns to be maintained in the encoding. The topological loss is defined following (Moor et al. 2020) as:

$$L_{X \rightarrow Z} := \frac{1}{2} \|A_X^{\pi_X} - A_Z^{\pi_X}\|^2, \quad (1)$$

$$L_{Z \rightarrow X} := \frac{1}{2} \|A_Z^{\pi_Z} - A_X^{\pi_Z}\|^2. \quad (2)$$

Here, $L_{X \rightarrow Z}$ and $L_{Z \rightarrow X}$ together form the topological loss $L_t = L_{X \rightarrow Z} + L_{Z \rightarrow X}$. For a mini-batch, X , \hat{X} , and Z denote the input, output, and latent spaces, respectively.

Persistent homology is then computed on both X and Z to extract topologically relevant distances, with π_X and π_Z denoting the persistence pairings that indicate which distances in A_X and A_Z are topologically significant. (i.e., indices of edges corresponding to topological features). Minimizing the combined objective Eq. 3 enforces topological consistency, ensuring that the latent space preserves the structure of the data space. In the ideal case, when the latent and data space topologies are perfectly aligned, both $L_{X \rightarrow Z}$ and $L_{Z \rightarrow X}$ vanish.

$$L := L_{\text{rec}}(X, \hat{X}) + \lambda L_t. \quad (3)$$

This term is added to the reconstruction loss of the autoencoder, where λ controls the strength of the topological regularization. Gradients are computed efficiently since pairings change only under substantial perturbations, ensuring loss differentiability during training. The output of the TopoAE is considered a purified representation, where the latent space captures topology-preserving features derived solely from persistent homology (Fig. 2). This process removes much of the adversarial perturbation in the input data, although the manifold reconstructed by the TopoAE is not fully aligned with classifier expectations. This motivates the role of the Reformer module in the pipeline.

The overall training objective for the Reformer combines three losses: a mean squared error loss \mathcal{L}_{MSE} for the pixel-level reconstruction between the TopoAE output and the VAE-reformed output, a cross-entropy loss \mathcal{L}_{CE} between classifier predictions (logits) on the VAE-reformed output and the ground-truth labels, and a KL divergence term \mathcal{L}_{KL} regularization. The MSE loss ensures the reconstruction remains structurally similar to the original image. In contrast, the cross-entropy loss encourages the Reformer to align the TopoAE output to the manifold expected by the classifier. The coefficients λ_1 , λ_2 , and λ_3 are the loss weights for each, respectively.

$$\mathcal{L} = \lambda_1 \mathcal{L}_{\text{MSE}} + \lambda_2 \mathcal{L}_{\text{CE}} + \lambda_3 \mathcal{L}_{\text{KL}} \quad (4)$$

The TopoReformer is trained separately on unperturbed samples from the training sets of MNIST (LeCun, Cortes, and Burges 2010), EMNIST (Cohen et al. 2017), and the OCR dataset (Belval 2020) until convergence, following (Moor et al. 2020). Afterward, its weights are frozen and used only for inference within the pipeline. The VAE and Auxiliary Module are then trained on the outputs of the TopoAE, namely, the latent vector and the topologically purified image, which are passed to the Auxiliary Module and VAE, respectively, using unperturbed inputs and the objective function in Eq. 4. The classifier weights remain fixed throughout training.

Auxiliary Training

The Auxiliary Module receives the latent representation produced by the TopoAE via a learned latent projection network. This design leverages the fact that the TopoAE encodes inputs into a topology-aware latent space, where unperturbed and adversarially perturbed inputs occupy similar

regions due to global manifold preservation. By feeding this representation to the Auxiliary Module, the Reformer can exploit this for more accurate predictions even under strong attacks. The auxiliary supervision component, when introduced independently, exhibits limited effectiveness, yielding marginal or inconsistent improvements across attack settings. This behavior primarily arises from *insufficient gradient propagation* to the auxiliary module, as the model tends to rely predominantly on the TopoReformer-purified output pathway rather than engaging with latent representations. A **Freeze-Flow training paradigm** is used to ensure proper training of the Auxiliary Module. Gradients are forcefully routed to it by first freezing the encoder of the Reformer VAE. After a set number of warmup epochs, the decoder is unfrozen, and the entire VAE and Auxiliary Module are trained jointly. The warmup phase ensures the auxiliary pathway receives stable gradients before the primary purified pathway dominates, effectively balancing optimization across both branches. This unified approach enables the auxiliary module to establish meaningful latent representations and improves robustness under stronger attacks.

Topological Latent Visualization

Fig. 2 illustrates the motivation behind using topological autoencoders for adversarial and downstream OCR tasks. Even when trained with moderate noise additions, the TopoReformer produces consistent and separable latent space representations Eq. (1), Eq. (2). The autoencoder (AE) preserves digit class separation in the latent space, with each color cluster corresponding to a distinct digit or character. As observed in the MNIST latent map (Fig. 2a), the clusters are clean and radially separable, whereas in EMNIST (Fig. 2b), they appear more entangled due to the higher class diversity. However, the separation remains discernible even for highly imbalanced datasets.

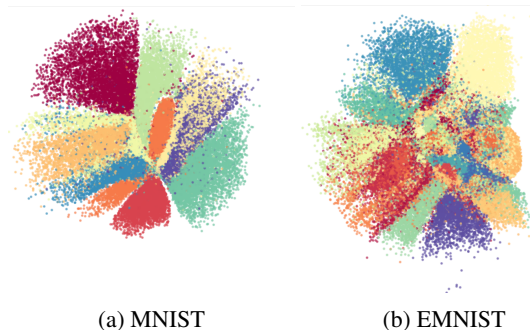


Figure 2: Comparison of topological latent visualizations.

Experimentation

This section is divided into four parts: Datasets, OCR model attack setup, the classifiers used to evaluate performance, and visualization of latent features learned by TopoReformer. The classifiers are trained using the total loss function in Eq. 3 with loss weights $\lambda_1 = 1$, $\lambda_2 = 0.5$, and $\lambda_3 = 0.5$. Training is performed using Adam optimizer (Kingma and Ba 2017) with a learning rate of 0.001.

Table 1: Ablation study under different L_∞ adversarial attacks on MNIST and EMNIST (reporting F1-score and Precision). Metrics are shown in percent (%). Attack strengths are shown in the confidence parameter (c) and perturbation budget (ϵ).

			MNIST		EMNIST	
Classical Attacks	Strength	Ablation	F1	Precision	F1	Precision
Carlini	Weak / Strong $c = 1e-2/1e+1$	No Defense	30.41 / 4.30	31.23 / 6.78	36.54 / 33.85	53.59 / 50.99
		+ TopoAE	53.92 / 48.51	61.35 / 50.68	30.87 / 27.71	66.00 / 64.10
		+ Reformer	65.38 / 67.93	71.11 / 69.83	50.64 / 49.16	59.71 / 58.29
		+ Aux	65.36 / 72.41	73.17 / 74.85	64.98 / 63.92	69.37 / 68.50
		+ Warmup	65.86 / 75.15	73.17 / 77.31	69.66 / 68.82	73.20 / 72.51
PGD	Weak / Strong $\epsilon = 0.005/0.01$	No Defense	96.74 / 96.62	96.90 / 96.69	84.87 / 72.66	85.66 / 74.54
		+ TopoAE	96.89 / 96.68	96.92 / 96.72	89.26 / 86.77	89.57 / 87.22
		+ Reformer	97.17 / 96.93	97.19 / 96.95	90.30 / 89.51	90.63 / 89.87
		+ Aux	97.60 / 97.62	97.62 / 97.64	83.25 / 82.75	84.79 / 84.31
		+ Warmup	97.70 / 97.62	97.72 / 97.64	84.53 / 83.79	85.12 / 84.43
FGSM	Weak / Strong $\epsilon = 0.005/0.01$	No Defense	96.87 / 96.61	96.89 / 96.65	90.83 / 72.59	91.04 / 73.83
		+ TopoAE	96.86 / 96.63	96.90 / 96.89	90.48 / 85.47	90.73 / 86.04
		+ Reformer	97.01 / 96.94	97.04 / 96.96	90.95 / 89.17	91.14 / 84.94
		+ Aux	97.60 / 97.21	97.62 / 97.62	90.49 / 83.60	90.73 / 89.41
		+ Warmup	97.69 / 97.51	97.71 / 97.71	90.48 / 84.42	90.72 / 85.00

Datasets

The evaluation is conducted on three benchmark datasets, OCR Dataset (Belval 2020; He et al. 2023), MNIST (LeCun, Cortes, and Burges 2010), and EMNIST (Cohen et al. 2017) letters. MNIST and EMNIST were chosen because their character sets closely resemble the inputs typically encountered by OCR models. Three classical adversarial attacks, PGD, FGSM, and Carlini, and two adaptive adversarial attacks, EOT and BPDA, are applied to the test sets, with classical attacks evaluated at both strong and weak strength levels. Comparisons are made against a self-constructed baseline, as existing benchmarks for classification under adversarial purification with topology-preserving autoencoders are limited. Strength levels for PGD and FGSM are selected as done in (Meng and Chen 2017). These works report performance on adversarial attack detection rather than classification tasks. For Carlini and other adaptive attacks, the strength is adjusted until classifier performance degrades, establishing a baseline on which components are added to demonstrate incremental improvements. The experimentation is extended to attacks specific to OCR models. The OCR training set was generated using the open-source code available here (Belval 2020). The dataset spans 53 classes, including uppercase and lowercase characters and a blank token. Unlike MNIST and EMNIST, this dataset is word-based, introducing additional structural challenges necessitating character-wise processing.

OCR Model Adversarial Attack Setup

FAWA (Chen, Sun, and Xu 2020) is a white-box, targeted attack tailored for OCR that embeds adversarial signals within plausible “watermark” overlays. By constraining perturba-

tions to visually natural overlays commonly seen in documents, FAWA achieves near-perfect attack success with substantially reduced perturbation magnitude and iterations compared to pixel-space baselines. Evaluations are shown using character-level performance and attack success rate (ASR), where a 100% ASR indicates that all adversarial images are misidentified as the targeted texts by the threat model. Table 3 summarizes the results. However, applying this directly to OCR words proved ineffective, as word-level images lack a consistent geometric structure. To address this, words were decomposed into individual characters. An auto-padding step was applied to ensure that all decomposed characters had a uniform size, as required by the model. Later, each character was centered with auto-padding to dimensions $2 \times 28 \times 44$. Following processing and purification at the character level, the characters were recombined into their original word-level format of 32×100 . This design allowed the pipeline to exploit character-level features even in word-based OCR, thereby preserving robustness and accuracy.

Classifier Architectures

The MNIST and EMNIST classifiers in the pipeline use the architectures as described in the Magnet (Meng and Chen 2017). The OCR architectures used in this work encompass CTC-based and attention-based designs to provide a broad evaluation of the proposed defense. The three CTC-based models CRNN (Shi, Bai, and Yao 2016), Rosetta (Borisyuk, Gordo, and Sivakumar 2018), and STAR-Net (Liu et al. 2016) combine convolutional feature extraction with sequence modeling and CTC-based decoding, differing in backbone complexity and feature aggregation. The

Table 2: Ablation study under adaptive adversarial attacks on MNIST and EMNIST datasets (reporting Attack Success Rate, F1-score, and Precision). Metrics are shown in percent (%).

Adaptive Attack	Defense	MNIST			EMNIST		
		ASR ↓	F1 ↑	Precision ↑	ASR ↓	F1 ↑	Precision ↑
EOT	No Defense	99.05	3.38	5.21	97.73	1.42	2.67
	TopoReformer	9.19	90.73	91.07	28.32	73.28	75.12
EOT+BPDA	No Defense	99.70	3.21	4.89	98.69	1.36	2.54
	TopoReformer	36.59	64.71	66.65	44.26	58.92	61.31
BPDA	No Defense	99.60	4.44	7.28	95.30	2.03	5.17
	TopoReformer	81.14	15.65	40.98	84.46	12.77	35.42

two attention-based models RARE (Shi et al. 2016) and TRBA (Baek et al. 2019) employ spatial attention and cross-entropy-based decoding to capture context and sequential dependencies, representing a complementary approach to CTC frameworks. Together, these architectures cover a representative spectrum of modern OCR pipelines.

Results

The proposed method is evaluated using quantitative and qualitative analyses to assess its robustness and interpretability. Quantitative results include ablation studies that isolate the contribution of each component. OCR-specific evaluations demonstrate the transferability of the defense to sequence-based recognition tasks. Qualitative analysis is through Grad-CAM visualizations (Selvaraju et al. 2017).

Quantitative Results

Classical Attacks Results Table 1 presents an ablation study evaluating the contributions of each architectural component under three adversarial attack scenarios on MNIST and EMNIST. Strength levels for PGD and FGSM follow the approach in (Meng and Chen 2017), while for the Carlini–Wagner (C&W) attack, the perturbation is adjusted until the classifier performs poorly. The standalone classifier exhibits significant vulnerability, achieving F1 scores of 30.41% on MNIST and 36.54% on EMNIST under weak C&W attacks. Incorporating TopoReformer substantially improves performance, raising F1 scores to 65.86% on MNIST and 69.66% on EMNIST. The demonstration of the complementary effect of the freeze flow training paradigm is also clearly seen; any anomaly in the ablations can be attributed to the manifold mismatch between the TopoReformer output and the classifier’s inputs. C&W generates minimal, high-confidence perturbations that reduce baseline accuracy to near zero (Carlini and Wagner 2017), leaving considerable room for corrective gains. In contrast, PGD and FGSM are first-order attacks that do not always succeed, resulting in higher baseline performance and correspondingly smaller absolute improvements. Prior studies have shown that iterative PGD and multi-step FGSM attacks often satu-

rate on standard datasets (Madry et al. 2017; Meng and Chen 2017), limiting the measurable effect of purification. Furthermore, TopoReformer enforces global manifold coherence rather than explicitly regularizing local gradients, making it particularly effective against fragile, low-distortion C&W perturbations while producing moderate gains for already strong FGSM and PGD attacks (Goodfellow, Shlens, and Szegedy 2014; Tramer et al. 2020) as seen above.

Adaptive Attack Results To avoid a false sense of security (Athalye, Carlini, and Wagner 2018) Table 2 shows TopoReformer’s behavior is analyzed under three adaptive settings (EOT, BPDA, EOT+BPDA). The model’s strong performance, particularly under EOT, indicates that its defense mechanism is not merely denoising or gradient obfuscation. (Tramer et al. 2020) emphasized that robust evaluation should expose not just whether a defense breaks but also how different adaptive strategies interact. Following this philosophy, while BPDA reduces the defense performance, EOT-based attacks are less effective, revealing how topological constraints reshape gradient landscapes. The proposed method integrates a topological autoencoder constraint into the latent space and achieves notable robustness against standard and adaptive attacks such as FGSM, C&W, and EOT. Interestingly, this robustness arises without explicit gradient regularization, suggesting that preserving global manifold topology implicitly constrains the model’s **Lipschitz continuity** (Tsuzuku, Sato, and Sugiyama 2018), that is, it limits how abruptly latent representations can vary in response to input perturbations. By maintaining the continuity and connectivity of the data manifold, the model resists large deformations in representation space, preserving class separation even under stochastic or expectation-based attacks. The model retains strong performance under EOT and EOT+BPDA attacks, indicating that the topological constraint promotes global stability and smooth transitions across the latent manifold. However, under BPDA alone, the defense weakens, consistent with the hypothesis that the topological regularizer enforces global Lipschitz-like smoothness but does not directly constrain fine-grained local curvature, which BPDA explicitly exploits. Overall,

Table 3: Ablation study of OCR-specific FAWA adversarial attack on diverse OCR Models. Metrics include Attack Success Rate (ASR, lower is better) and character-level performance (higher is better). All metrics are shown in percent (%).

Model Type	Model	Defense	ASR ↓	Char Accuracy ↑	Char Precision ↑
CTC-based	CRNN	No Defense	100	48.13	45.69
		Defense	78.83	71.00	71.61
	Rosetta	No Defense	99.83	69.66	62.94
		Defense	44.08	85.98	87.52
	STAR-Net	No Defense	98.92	74.52	69.77
		Defense	65.17	79.81	81.44
Attention-based	RARE	No Defense	99.92	51.25	49.77
		Defense	87.67	65.18	64.74
	TRBA	No Defense	99.83	46.68	44.26
		Defense	60.75	80.26	80.81

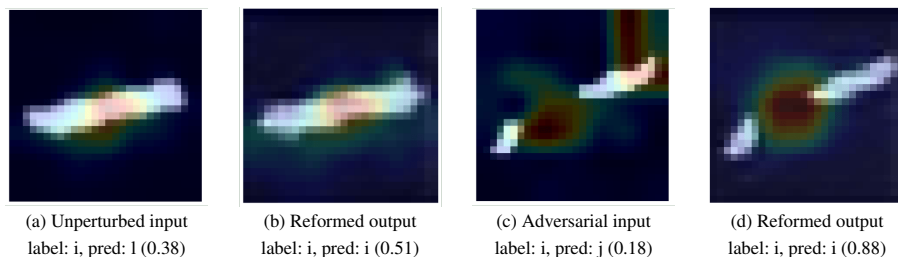


Figure 3: Comparison of Grad-CAM visualizations. (a)–(b) Unperturbed images, (c)–(d) adversarial images. Reformers project inputs toward topology-consistent manifolds, leading to more focused and confident class-discriminative regions.

these results highlight that topology-based regularization enhances global geometric consistency, offering a complementary axis of robustness that operates at the manifold level rather than through explicit gradient control. Furthermore, the classifiers maintain approximately 98% accuracy on MNIST and 94% on EMNIST in unperturbed (clean) settings. The negligible variation in unperturbed performance confirms that the unified TopoReformer pipeline enhances adversarial robustness without compromising standard classification capability.

OCR Ablation Results Table 3 summarizes the OCR-specific adversarial defense evaluation conducted across five representative architectures: three CTC-based models, CRNN, Rosetta, and STAR-Net using CTC loss, and two attention-based models, RARE and TRBA, using cross-entropy loss. Each model is evaluated under two configurations: the baseline *No Defense* setup and the proposed *TopoReformer* configuration. Baseline OCR models demonstrate complete vulnerability to adversarial perturbations, with ASR values near 100% and considerable drops in character accuracy (e.g., 48.13% for CRNN). Incorporating the TopoReformer module substantially enhances robustness across all architectures, consistently reducing ASR and improving accuracy, precision, and recall. For instance, in the CRNN model, the ASR drops to 78.83% while accuracy increases to 71%, and similar gains are observed for

the other models. Even though adding the Reformer component yielded notable improvements in MNIST and EMNIST experiments, it was intentionally excluded from OCR evaluations to preserve deployability efficiency.

Qualitative Results

To interpret the effect of the topological constraint, Grad-CAM is used (Selvaraju et al. 2017) to visualize how the model’s attention changes under adversarial perturbations. Grad-CAM produces a spatial heatmap highlighting the most influential regions for prediction. Fig. 3 compares the baselines and TopoReformer’s attention maps. The baseline shows scattered or shifted activations under adversarial noise, often focusing on irrelevant regions. TopoReformer maintains compact, semantically consistent activations, concentrating on the object of interest even under perturbation. Another noteworthy observation is that the confidence scores of unperturbed images also increase after being processed through the TopoAE. This is particularly interesting, as most adversarial training techniques tend to improve robustness at the expense of performance on unperturbed samples. These results support the hypothesis that enforcing topological consistency in the latent manifold encourages globally coherent and stable attention, reducing representational drift.

Conclusion

This work demonstrates that topological feature analysis and persistent homology-based purification form a viable defense pipeline. Experimental results on MNIST and EMNIST demonstrate that TopoReformer substantially outperforms baseline classifiers under standard adversarial attacks such as FGSM, PGD, and C&W. It also remains effective against adaptive attacks like EOT and EOT+BPDA, as well as OCR-specific threats, including FAWA watermark-based perturbations. By leveraging the inherent stability of topological representations, TopoReformer preserves the global structure of the data manifold, naturally filtering out adversarial noise and maintaining semantic integrity. These results consistently reduce attack success rates and improve robustness across all evaluated metrics, highlighting the effectiveness of topology-driven purification under both standard and adaptive adversarial settings.

Future Work

Future work will focus on integrating topology-aware training directly into OCR model optimization, thereby removing the need for a separate Reformer stage. Another direction involves constructing a comprehensive benchmark dataset and standardized classifier suite for the evaluation of OCR-specific adversarial attacks and solutions. This benchmark will encompass both classical and adaptive threat models, addressing the current gap in publicly available resources for OCR robustness assessment.

References

- Akhtar, N.; and Mian, A. 2018. Threat of adversarial attacks on deep learning in computer vision: A survey. *Ieee Access*, 6: 14410–14430.
- Athalye, A.; Carlini, N.; and Wagner, D. 2018. Obfuscated gradients give a false sense of security: Circumventing defenses to adversarial examples. In *International conference on machine learning*, 274–283. PMLR.
- Athalye, A.; Engstrom, L.; Ilyas, A.; and Kwok, K. 2018. Synthesizing robust adversarial examples. In *International conference on machine learning*, 284–293. PMLR.
- Baek, J.; Kim, G.; Lee, J.; Park, S.; Han, D.; Yun, S.; Oh, S. J.; and Lee, H. 2019. What is wrong with scene text recognition model comparisons? dataset and model analysis. In *Proceedings of the IEEE/CVF international conference on computer vision*, 4715–4723.
- Bakhti, Y.; Fezza, S. A.; Hamidouche, W.; and Déforges, O. 2019. DDSA: A defense against adversarial attacks using deep denoising sparse autoencoder. *IEEE Access*, 7: 160397–160407.
- Bazzo, G. T.; Lorentz, G. A.; Suarez Vargas, D.; and Moreira, V. P. 2020. Assessing the impact of OCR errors in information retrieval. In *European Conference on Information Retrieval*, 102–109. Springer.
- Belval. 2020. TextRecognitionDataGenerator. <https://github.com/Belval/TextRecognitionDataGenerator>. Accessed: 30 August 2025.
- Borisyuk, F.; Gordo, A.; and Sivakumar, V. 2018. Rosetta: Large scale system for text detection and recognition in images. In *Proceedings of the 24th ACM SIGKDD international conference on knowledge discovery & data mining*, 71–79.
- Carlini, N.; and Wagner, D. 2017. Towards evaluating the robustness of neural networks. In *2017 IEEE Symposium on Security and Privacy (SP)*, 39–57. Ieee.
- Chakraborty, A.; Alam, M.; Dey, V.; Chattopadhyay, A.; and Mukhopadhyay, D. 2021. A survey on adversarial attacks and defences. *CAAI Transactions on Intelligence Technology*, 6(1): 25–45.
- Chen, L.; Sun, J.; and Xu, W. 2020. FAWA: Fast adversarial watermark attack on optical character recognition (OCR) systems. In *Joint European Conference on Machine Learning and Knowledge Discovery in Databases*, 547–563. Springer.
- Chen, Y.-C.; and Lu, C.-S. 2025. Adversarial Masked Autoencoder Purifier with Defense Transferability. *arXiv preprint arXiv:2501.16904*.
- Cintas, C.; Speakman, S.; Akinwande, V.; Ogallo, W.; Weldemariam, K.; Sridharan, S.; and McFowland, E. 2021. Detecting adversarial attacks via subset scanning of autoencoder activations and reconstruction error. In *Proceedings of the twenty-ninth international conference on international joint conferences on artificial intelligence*, 876–882.
- Cohen, G.; Afshar, S.; Tapson, J.; and van Schaik, A. 2017. EMNIST: an extension of MNIST to handwritten letters. *arXiv:1702.05373*.
- Cohen-Steiner, D.; Edelsbrunner, H.; and Harer, J. 2005. Stability of persistence diagrams. In *Proceedings of the twenty-first annual symposium on Computational geometry*, 263–271.
- Dhillon, G. S.; Azizzadenesheli, K.; Lipton, Z. C.; Bernstein, J.; Kossaifi, J.; Khanna, A.; and Anandkumar, A. 2018. Stochastic activation pruning for robust adversarial defense. *arXiv preprint arXiv:1803.01442*.
- Edelsbrunner, H.; Harer, J.; et al. 2008. Persistent homology—a survey. *Contemporary mathematics*, 453(26): 257–282.
- Folz, J.; Palacio, S.; Hees, J.; and Dengel, A. 2020. Adversarial defense based on structure-to-signal autoencoders. In *2020 IEEE Winter Conference on Applications of Computer Vision (WACV)*, 3568–3577. IEEE.
- Gebhart, T.; and Schrater, P. 2017. Adversary detection in neural networks via persistent homology. *arXiv preprint arXiv:1711.10056*.
- Goibert, M.; Ricatte, T.; and Dohmatob, E. 2022. An adversarial robustness perspective on the topology of neural networks. *arXiv preprint arXiv:2211.02675*.
- Goodfellow, I. J.; Shlens, J.; and Szegedy, C. 2014. Explaining and harnessing adversarial examples. *arXiv preprint arXiv:1412.6572*.
- Guo, C.; Rana, M.; Cisse, M.; and Van Der Maaten, L. 2017. Countering adversarial images using input transformations. *arXiv preprint arXiv:1711.00117*.

- He, Y.; Chen, K.; Chen, G.; Ma, Z.; Zhang, K.; Zhang, J.; Bian, H.; Fang, H.; Zhang, W.; and Yu, N. 2023. ProTegO: Protect text content against OCR extraction attack. In *Proceedings of the 31st ACM International Conference on Multimedia*, 7424–7434.
- He, Z.; Yang, Y.; Chen, P.-Y.; Xu, Q.; and Ho, T.-Y. 2022. Be your own neighborhood: Detecting adversarial example by the neighborhood relations built on self-supervised learning. *arXiv preprint arXiv:2209.00005*.
- Horn, M.; De Brouwer, E.; Moor, M.; Moreau, Y.; Rieck, B.; and Borgwardt, K. 2021. Topological graph neural networks. *arXiv preprint arXiv:2102.07835*.
- Hwang, U.; Park, J.; Jang, H.; Yoon, S.; and Cho, N. I. 2019. Puvae: A variational autoencoder to purify adversarial examples. *IEEE Access*, 7: 126582–126593.
- Imam, N. H.; Vassilakis, V. G.; and Kolovos, D. 2022. OCR post-correction for detecting adversarial text images. *Journal of Information Security and Applications*, 66: 103170.
- Kakani, B. V.; Gandhi, D.; and Jani, S. 2017. Improved OCR based automatic vehicle number plate recognition using features trained neural network. In *2017 8th international conference on computing, communication and networking technologies (ICCCNT)*, 1–6. IEEE.
- Kalaria, D.; Hazra, A.; and Chakrabarti, P. P. 2022. Towards adversarial purification using denoising autoencoders. *arXiv preprint arXiv:2208.13838*.
- Karhikeyan, S.; de Herrera, A. G. S.; Doctor, F.; and Mirza, A. 2021. An OCR post-correction approach using deep learning for processing medical reports. *IEEE Transactions on Circuits and Systems for Video Technology*, 32(5): 2574–2581.
- Kingma, D. P.; and Ba, J. 2017. Adam: A Method for Stochastic Optimization. *arXiv:1412.6980*.
- Kuang, H.; Liu, H.; Lin, X.; and Ji, R. 2024. Defense against adversarial attacks using topology aligning adversarial training. *IEEE Transactions on Information Forensics and Security*, 19: 3659–3673.
- LeCun, Y.; Cortes, C.; and Burges, C. 2010. MNIST handwritten digit database. *ATT Labs [Online]*. Available: <http://yann.lecun.com/exdb/mnist, 2>.
- Li, Y.; Cheng, M.; Hsieh, C.-J.; and Lee, T. C. 2022. A review of adversarial attack and defense for classification methods. *The American Statistician*, 76(4): 329–345.
- Liu, W.; Chen, C.; Wong, K.-Y. K.; Su, Z.; and Han, J. 2016. Star-net: a spatial attention residue network for scene text recognition. In *BMVC*, volume 2, 7.
- Lu, P.-H.; Chen, P.-Y.; Chen, K.-C.; and Yu, C.-M. 2018. On the limitation of MagNet defense against L1-based adversarial examples. In *2018 48th Annual IEEE/IFIP International Conference on Dependable Systems and Networks Workshops (DSN-W)*, 200–214. IEEE.
- Madry, A.; Makelov, A.; Schmidt, L.; Tsipras, D.; and Vladu, A. 2017. Towards deep learning models resistant to adversarial attacks. *arXiv preprint arXiv:1706.06083*.
- Meng, D.; and Chen, H. 2017. Magnet: a two-pronged defense against adversarial examples. In *Proceedings of the 2017 ACM SIGSAC conference on computer and communications security*, 135–147.
- Moor, M.; Horn, M.; Rieck, B.; and Borgwardt, K. 2020. Topological autoencoders. In *International conference on machine learning*, 7045–7054. PMLR.
- Ngairangbam, V. S.; Rozwoda, B.; Sakurai, K.; and Spannowsky, M. 2025. Enhancing anomaly detection with topology-aware autoencoders. *arXiv:2502.10163*.
- Pingili, R. 2025. AI-driven intelligent document processing for banking and finance. *International Journal of Management & Entrepreneurship Research*, 7(2): 98–109.
- Qian, Z.; Huang, K.; Wang, Q.-F.; and Zhang, X.-Y. 2022. A survey of robust adversarial training in pattern recognition: Fundamental, theory, and methodologies. *Pattern Recognition*, 131: 108889.
- Sainburg, T.; McInnes, L.; and Gentner, T. Q. 2021. Parametric UMAP embeddings for representation and semisupervised learning. *Neural Computation*, 33(11): 2881–2907.
- Selvaraju, R. R.; Cogswell, M.; Das, A.; Vedantam, R.; Parikh, D.; and Batra, D. 2017. Grad-cam: Visual explanations from deep networks via gradient-based localization. In *Proceedings of the IEEE international conference on computer vision*, 618–626.
- Shi, B.; Bai, X.; and Yao, C. 2016. An end-to-end trainable neural network for image-based sequence recognition and its application to scene text recognition. *IEEE transactions on pattern analysis and machine intelligence*, 39(11): 2298–2304.
- Shi, B.; Wang, X.; Lyu, P.; Yao, C.; and Bai, X. 2016. Robust scene text recognition with automatic rectification. In *Proceedings of the IEEE conference on computer vision and pattern recognition*, 4168–4176.
- Tramer, F.; Carlini, N.; Brendel, W.; and Madry, A. 2020. On adaptive attacks to adversarial example defenses. *Advances in neural information processing systems*, 33: 1633–1645.
- Tsuzuku, Y.; Sato, I.; and Sugiyama, M. 2018. Lipschitz-margin training: Scalable certification of perturbation invariance for deep neural networks. *Advances in neural information processing systems*, 31.
- Vu, M.; Zollicoffer, G.; Mai, H.; Nebgen, B.; Alexandrov, B.; and Bhattarai, M. 2025. Topological Signatures of Adversaries in Multimodal Alignments. *arXiv preprint arXiv:2501.18006*.
- Xie, C.; Wang, J.; Zhang, Z.; Ren, Z.; and Yuille, A. 2017. Mitigating adversarial effects through randomization. *arXiv preprint arXiv:1711.01991*.
- Yang, Z.; Xu, Z.; Zhang, J.; Hartley, R.; and Tu, P. 2024. Adversarial purification with the manifold hypothesis. In *Proceedings of the AAAI Conference on Artificial Intelligence*, volume 38, 16379–16387.
- Zhao, W.; Alwidian, S.; and Mahmoud, Q. H. 2022. Adversarial training methods for deep learning: A systematic review. *Algorithms*, 15(8): 283.
- Zomorodian, A.; and Carlsson, G. 2004. Computing persistent homology. In *Proceedings of the twentieth annual symposium on Computational geometry*, 347–356.